ESC European Society of Cardiology

Cardiovascular Research (2019) **115**, 1804–1810
doi:10.1093/cvr/cvz063

Therapeutic modulation of RNA-binding protein Rbm38 facilitates re-endothelialization after arterial injury

Kristina Sonnenschein[1,2], Jan Fiedler[1], Angelika Pfanne[1], Annette Just[1], Saskia Mitzka[1], Robert Geffers[3], Andreas Pich[4], Johann Bauersachs[2,5], and Thomas Thum[1,5,6]*

[1]Institute of Molecular and Translational Therapeutic Strategies (IMTTS), Hannover Medical School, Carl-Neuberg-Strasse 1, 30625 Hannover, Germany; [2]Department of Cardiology and Angiology, Hannover Medical School, Hannover, Germany; [3]Helmholtz Centre for Infection Research, Braunschweig, Germany; [4]Institute of Toxicology, Hannover Medical School, Hannover, Germany; [5]Excellence Cluster REBIRTH, Hannover Medical School, Hannover, Germany; and [6]National Heart and Lung Institute, Imperial College London, London, UK

Received 20 June 2018; revised 13 December 2018; editorial decision 28 February 2019; accepted 1 March 2019; online publish-ahead-of-print 7 March 2019

Time for primary review: 43 days

Aims Delayed re-endothelialization after balloon angioplasty in patients with coronary or peripheral artery disease impairs vascular healing and leads to neointimal proliferation. In the present study, we examined the effect of RNA-binding motif protein 38 (Rbm38) during re-endothelialization in a murine model of experimental vascular injury.

Methods and results Left common carotid arteries of C57BL/6 mice were electrically denudated and endothelial regeneration was evaluated. Profiling of RNA-binding proteins revealed dysregulated expression of Rbm38 in the denudated and regenerated areas. We next tested the importance of Rbm38 in human umbilical vein endothelial cells (HUVECS) and analysed its effects on cellular proliferation, migration and apoptosis. Rbm38 silencing *in vitro* demonstrated important beneficial functional effects on migratory capacity and proliferation of endothelial cells. *In vivo,* local silencing of Rbm38 also improved re-endothelialization of denuded carotid arteries. Luciferase reporter assay identified miR-98 and let-7f to regulate Rbm38 and the positive proliferative properties of Rbm38 silencing *in vitro* and *in vivo* were mimicked by therapeutic overexpression of these miRNAs.

Conclusion The present data identified Rbm38 as an important factor of the regulation of various endothelial cell functions. Local inhibition of Rbm38 as well as overexpression of the upstream regulators miR-98 and let-7f improved endothelial regeneration *in vivo* and thus may be a novel therapeutic entry point to avoid endothelial damage after balloon angioplasty.

Keywords RNA-binding protein Rbm38 • Vascular injury • Re-endothelialization

1. Introduction

RNA-binding proteins (RBPs) have emerged as important regulators of multiple cellular pathways. Specifically, RBPs control several functions of RNAs such as biogenesis, stability and activity.[1] RBPs play an important role in the post-transcriptional regulation of gene expression by regulating different processes of non-coding RNA translation and metabolism.[2] One of the regulating partners of RBPs is the group of small non-coding RNAs called microRNAs (miRNAs). miRNAs are key players in post-transcriptional regulation of gene expression. Specific miRNA expression patterns correlate with diverse cardiovascular diseases, e.g. cardiac hypertrophy, heart failure, and vascular remodelling.[3] New aspects of miRNA overexpression and silencing in mice reveal pathogenic and protective properties of miRNAs *in vivo*.[4,5] However, still little is known about the transcriptional regulation of miRNAs and the importance of RBPs in the vascular system.

This is of importance, as certain RBPs, such as the RNA-binding motif protein 38 (Rbm38), have been reported to also control processes in the cell cycle. Rbm38 induces the cell cycle arrest in G1-phase by stabilizing the messenger RNA (mRNA) of p21.[6–8] In several tumours Rbm38 displayed different functions: in some cancer types it acts as a tumour suppressor,[9–11] whereas in others its overexpression is associated with poor clinical outcome by influencing, e.g. the drug and radiation resistance.[12] Somatic Rbm38 knockout (-/-) mice expressed haematopoietic

* Corresponding author. Tel: +49 511 532 5272; fax: +49 511 532 5274, E-mail: Thum.Thomas@mh-hannover.de

defects[13,14] and loss of Rbm38 lead to T-cell lymphomagenesis.[15] Also the role of Rbm38 on cardiac remodelling was recently examined,[14] but the function of Rbm38 in endothelial cells is still unclear.

The endothelium features an important role in the development of atherosclerosis and related diseases. Endothelial dysfunction is associated with the loss of protective properties and pro-thrombotic and pro-inflammatory features.[16,17] A special type of endothelial dysfunction occurs in the context of vascular healing and remodelling after balloon angioplasty and stent implantation. Coronary or peripheral interventions are associated with arterial injury that leads to endothelial dysfunction. Attenuated re-endothelialization of the vessels after an arterial injury intensifies the vascular inflammation reaction, impairs subsequent vascular healing and contributes to the development of neointimal proliferation and resulting restenosis.

In this study, we investigated the effect of Rbm38 modulation on endothelial cells and tested its potential therapeutic use after an arterial injury.

2. Methods

2.1 Cell culture

Human umbilical vein endothelial cells (HUVECs) were purchased from Lonza and cultured in EBM-2 (Lonza) supplemented with VEGF, hEGF, hydrocortisone, hFGF-B, R^3-IGF-1, gentamicin/amphotericin-B, ascorbic acid and 10% FBS under standard cell culture conditions (37°C, 5% CO_2).

HEK293T cells were cultured in DMEM medium (Gibco, Invitrogen, Germany) supplemented with 10% FBS and 1% Pen/Strep under standard cell culture conditions.

2.2 Transfection experiments (siRNA, pre-miRNA)

Transient liposomal transfection of cells was performed at a confluence of 60–70% 1 day after seeding. Final concentration of oligonucleotides was 150 nM for siRNA and 100 nM for pre-miRNA. Oligonucleotides that were used for transfection experiments were as following: siRNA Rbm38 (Santa Cruz sc-76368), control siRNA (Santa Cruz sc-37007), pre-miR-98 (Applied Biosystems, USA, AM 17100 PM 10426), and pre-miR-let7f (Applied Biosystems AM 17100 PM 10902). Specific siRNAs/miRNAs or control siRNAs/miRNAs and Lipofectamine 2000 (Invitrogen) were mixed separately with Opti-MEM I media (Invitrogen) and incubated for 5 min, then mixed together and incubated again for 20 min. For the transfection reaction serum-free conditions were applied and after 4 h medium was renewed. After 48 h cells were harvested and analysed. Silencing of proteins was monitored for 48 h after transfection by Western blot analysis.

2.3 Migration assay: Boyden chamber, scratch wounding assay

For Boyden-chamber migration treated endothelial cells were incubated with DAPI for 2 h, pelleted and resuspended in EBM-2 with 0.1% BSA and seeded on fibronectin-coated trans-well inserts (BD Biosciences, USA). Inserts were placed in wells containing chemoattractants (VEGF 5 ng/mL, SDF 100 ng/mL). Three images per well and replicate were performed after 2 h, and number of migrated cells was counted using NIS-elements DR software.

For the scratch wounding assay the migration capacity of transfected cells was analysed using culture-inserts (Ibidi, Germany). 15 000 HUVECs were placed to each side of culture-inserts 24 h after transfection. Twenty-four hours later, plastic patches were removed and two microscopic images per well were performed after 0, 4, 6, and 24 h. Wound area was calculated by the use of NIS-elements BR software (Nikon, Germany). Migration index was calculated by the following formula: area (0 h) - area (6 h)/area (0 h).

2.4 Cell proliferation assays: WST-1 viability assay

HUVECs were seeded in 96-well cell culture plates and transfected with siRNA/pre-miR 1 day after seeding. Proliferative capacity in siRNA/pre-miR-modulated cells, a WST-1 proliferation assay (Roche, Germany) was applied. Twenty-four hours after transfection medium was replaced by a starvation medium containing 0, 1% FCS, and without supplements for additional 24 h. Forty-eight hours after transfection medium was changed and replaced by medium containing WST-1 reagent according to the manufacturer's instructions. Then, WST-1 absorbance was measured at 450 nm.

2.5 Apoptosis staining

Transfected HUVECs were subjected to Annexin V/7-AAD staining applying FlowCellect Annexin Red Kit (Merck Millipore, Germany) and analysed on a Guava easyCyte (Merck Millipore). Apoptotic cells were considered to be Annexin V positive and 7-AAD negative.

2.6 Cell cycle assay

Cell cycle analysis was performed by the use of Guava Cell Cycle staining kit (Millipore, Germany) according to the manufacturer's instructions. Therefore, cells were transferred to a 96-well round bottom plates and fixed with cold 70% ethanol. Following the cells were stained with the Guava Cell Cycle Reagent and subjected to FACS analysis.

2.7 Real-time PCR analysis

RNA isolation was performed with TriFast reagent (Peqlab, China) according to the manufacturer's instructions. For detection of miRNAs in samples, specific TaqMan assays (Applied Biosystems) were applied. The small RNA molecule U6 small nuclear (RNU6-B) was amplified as a control. mRNA expression of GAPDH, Rbm38, and p21 was analysed by SYBR Green method using the following primers: GAPDH(f) 5' CCA GGCGCCCAATACG3', (r) 5' CCACATCGCTCAGACACCAT3'; p21(f) 5' GCAGACCAGCATGACAGATTTC3', (r) 5' GGATTAGGG CTTCCTCTTGGA3'. Primer for human Rbm38 was purchased Quantitect primer set (Qiagen QT00030576). Reverse transcription-polymerase chain reaction analysis was performed in an ICycler (BioRad, Germany). Microarray analysis was performed with Human Gene 1.0 ST (Affymetrix Systems, USA).

2.8 Western blotting experiments

10–30 μg of total protein were separated by SDS-PAGE, transferred to PVDF membrane and analysed by western blotting using standard protocols. The following antibodies were used to detect antigens: Rbm38 (Aviva Systems Biology, USA, ARP 40862_P050), p21 (Abcam, UK, ab109520), GAPDH (Abcam, ab8245) and CREB (Cell Signaling Technology, USA, #9197). Luminol reagent was used to detect the signals on the membrane using X-ray films (Kodak, Germany). Band intensity was calculated applying ImageJ software.

2.9 Luciferase reporter assay

Mir-98 and let-7f were identified as putative targets of Rbm38 using TargetScan database (http://www.targetscan.org). A luciferase reporter assay system was applied to validate potential Rbm38 targets as described previously.[3] A putative 3'UTR Rbm38 binding sequence was cloned into the cloning site of pMIR-REPORT vector (Ambion, USA). The resulting construct was co-transfected with the miRNAs of interest and β-galactosidase control plasmid (Promega, Germany) into HEK293 reporter cells in 48-well plates using Lipofectamine 2000 (Invitrogen). A total of 0.1 µg of plasmid DNA and 100 nmol/L miRNA was applied. Cells were incubated for 24 h before luciferase and ß-galactosidase activity was measured (Promega).

2.10 Immunoprecipitation experiments

HUVECs underwent immunoprecipitation (IP) using mouse control IgG (Santa Cruz, USA, sc-2025). For IP, antibodies were coupled to Dynabeads™ (Invitrogen). 10 million cells were used for IP and separated for control and Rbm38 pulldown group.

2.11 Immunohistochemistry

Rbm38-staining in HUVECs was performed to analyse cellular Rbm38 localization. HUVECs were washed with PBS and fixed with 4% paraformaldehyde (Roth) in PBS for 15 min at room temperature (RT). Cells were washed with PBS for 5 min at RT and permeabilized with 0.1% (v/v) Triton X-100 (Roth) in PBS for 10 min at 4°C. Then cells were washed with PBS for 5 min at RT for three times. After the washing procedure cells were incubated with donkey serum (5% v/v) for 30 min at RT. Cells were labelled with 1:100 dilution of specific primary antibody (Rbm38, Aviva ARP40862, Aviva Systems Biology) diluted 1:100 in donkey serum (5% v/v) at 4°C overnight. Unbound antibody was removed by washing the cells as previous described, followed by incubation with a 1:500 dilution of appropriate Alexa fluorophore secondary antibody (Alexa Fluor 488 Donkey-anti-rabbit IgG, A21206, Invitrogen) and a 1:1000 dilution of DAPI (Sigma-Aldrich, Germany) diluted in donkey serum (5% v/v) for 30 min at RT in the dark. The cells were washed with PBS for 5 min at RT for three times in the dark, leaving 500 µL PBS in each well. Cells were examined by fluorescence microscopy and images were taken.

2.12 Sample preparation for mass spectrometry and data analysis

10µg total protein of siRNA-modulated HUVECs used for IP were alkylated with acrylamide as described elsewhere[18] separated by 4–15% Mini-PROTEAN® TGX™ Precast Protein Gel (BioRad) and stained in Coomassie solution for 45 min at RT. Subsequently, the gel was destained (1 h or o/n) until the background was clear and protein bands were visible. Gel lanes containing complex samples were cut into pieces and proteins were in-gel digested using trypsin and extracted peptides were subjected to LC-MS analysis as described.[18] Briefly, protein containing gel pieces were destained two times with 200 µL 50% ACN, 50 mM ammonium bicarbonate (ABC) at 37°C for 30 min, and then dehydrated with 100% ACN. Solvent was removed in a vacuum centrifuge and 100 µL 10 ng/µL sequencing grade Trypsin (Promega) in 10% ACN, 40 mM ABC were added. Gels were rehydrated in trypsin solution for 1 h on ice and then covered with 10% ACN, 40 mM ABC. Digestion was performed over night at 37°C and was stopped by adding 100 µL of 50% ACN, 0, 1% TFA. After incubation at 37°C for 1 h the solution was transferred into a fresh sample vial. This step was repeated twice and extracts were combined and dried in a vacuum centrifuge. Dried peptide extracts were redissolved in 30 µL 2% ACN, 0.1% TFA with shaking at 800 rpm for 20 min. After centrifugation at 20 000×*g* aliquots of 12.5 µL each were stored at -20°C.

Peptide samples were separated with a nano-flow ultra-high pressure liquid chromatography system (RSLC, Thermo Scientific, Germany) equipped with a trapping column (3-µm C18 particle, 2 cm length, 75 µm ID, Acclaim PepMap, Thermo Scientific) and a 50-cm long separation column (2 µm C18 particle, 75 µm ID, Acclaim PepMap, Thermo Scientific). Peptide mixtures were injected, enriched, and desalted on the trapping column at a flow rate of 6 µL/min with 0.1% TFA for 5 min. The trapping column was switched online with the separating column and peptides were eluted with a multi-step binary gradient: linear gradient of buffer B (80% ACN, 0.1% formic acid) in buffer A (0.1% formic acid) from 4 to 25% in 30 min, 25 to 50% in 10 min, 50 to 90% in 5 min, and 10 min at 90% B. The column was reconditioned to 4% B in 15 min. The flow rate was 250 nL/min, and the column temperature was set to 45°C. The RSLC system was coupled online via a Nanospray Flex Ion Source II (Thermo Scientific) to an LTQ-Orbitrap Velos mass spectrometer. Metal-coated fused-silica emitters (SilicaTip, 10 µm i.d., New Objectives) and a voltage of 1.3 kV were used for the electrospray. Overview scans were acquired at a resolution of 60k in a mass range of m/z 300–1600 in the orbitrap analyzer and stored in profile mode. The top 10 most intensive ions of charges two or three and a minimum intensity of 2000 counts were selected for CID fragmentation with a normalized collision energy of 38.0, an activation time of 10 ms and an activation Q of 0.250 in the LTQ. Fragment ion mass spectra were recorded in the LTQ at normal scan rate and stored as centroid m/z value and intensity pairs. Active exclusion was activated so that ions fragmented once were excluded from further fragmentation for 70 s within a mass window of 10 ppm of the specific m/z value.

Raw data were processed with MaxQuant software (version 1.5.3.30)[19] and peptides were identified by searching against all human entries of the UniProtKB/Swiss-Prot database using the Andromeda search engine.[20] Propionamidation (C) was set as fixed modification and a maximum of two missed cleavages was allowed. Oxidation (M), deamidation (N/Q), and acetylation (protein N-terminal) were set as variable modifications. A false discovery rate of 0.01 on peptide and protein level was used for identification and 're-quantify' and 'match between runs' options were checked. Data were analysed and visualized with the software tools Perseus (version 1.5.2.6) and if applicable two sided one-sample Student's *t*-test was applied for comparison.[21]

2.13 Animals

All animal experiments were performed in male C57BL/6N mice (10–12 week old) in accordance with the guidelines from Directive 2010/63/EU of the European Parliament on the protection of animals used for scientific purposes and were approved by the Lower Saxony's regional office for consumer protection and food safety. At the end of *in vivo* experiments, mice were sacrificed by cervical dislocation for tissue sampling.

2.14 *In vivo* re-endothelialization assay

To study the *in vivo* effects of Rbm38 as well as miR-98 and let-7f, we performed the carotid artery injury as described previously.[22–24] In brief, animals were anaesthetized with ketamine (100 mg/kg IP) and xylazine (5 mg/kg IP). The electric injury was performed at the left common carotid artery of male C57BL/6 mice with a bipolar microregulator (ICC50, ERBE-Elektromedizin GmbH, Tuebingen, Germany). An electric

current of 2 W was applied for 2 s to each mm of carotid artery over a total length of exactly 4 mm with the use of a size marker parallel to the carotid artery. About 50–100µL of the appropriate siRNA or pre-miR were applied perivascular after the carotid injury in a thermoreversible pluronic gel (Pluronic gel F-127, Sigma). At 4°C pluronic gel is soluble and can be mixed with miRNAs or siRNAs of interest and becomes solid at RT shortly after application. Three days after carotid injury, endothelial regeneration was evaluated by staining denuded areas with 50 µL of solution containing 5% Evans blue dye via tail vein injection. The re-endothelialized area was calculated as the difference between the injured area and the blue-stained area by computer-assisted morphometric analysis. This model has been shown to allow accurate quantification of re-endothelialization.[23]

2.15 Statistical analysis

Statistical analysis was performed using GraphPad Prism (Version 4). Experimental analysis was performed in biological replicates from independent experiments and all values are expressed as mean ± SEM. Unpaired Student's *t*-test was used to compare two groups and one-way ANOVA with *post hoc* Tukey's test was used to calculate significant difference between ≥3 groups. A value of $P < 0.05$ was considered as statistically significant.

3. Results

3.1 Rbm38 is dynamically regulated during the endothelial healing process

RNA binding proteins have emerged as crucial players in the regulation of multiple cellular pathways as well as coding and non-coding RNAs. We thus initially screened expression of an array of important RNA-binding/modulating proteins in a translationally important disease model of carotid injury. Specifically, we investigated changes of expression of 13 RBPs after carotid injury and re-endothelialization. Most importantly, we found the RNA-binding motif protein Rbm38 to be highly upregulated during the injury process, but found normalization during the re-endothelialization process (*Figure 1A*, Supplementary material online, *Figure S1* and *Table S1*). We thus assumed the dynamic regulation of Rbm38 to be involved in endothelial healing. Especially the reduction of expression during the healing phase prompted us to speculate that silencing of Rbm38 could be beneficial for endothelial cell function.

3.2 Silencing of Rbm38-activated endothelial cells in vitro and improved re-endothelialization in vivo

To study the biological role of Rbm38 in endothelial cells we performed several *in vitro* assays. Silencing of Rbm38 led to a significant reduction of Rbm38 mRNA and protein levels (Supplementary material online, *Figure S2A, B*) and increased the migratory capacity of HUVECs (*Figure 1B*) as well as proliferative capacity (*Figure 1C*) and enhanced expression of cell cycle gene CDK6 (*Figure 1D*). In contrast, the apoptosis rate of HUVECs was not affected (Supplementary material online, *Figure S3*). Control siRNA or siRNA targeting Rbm38 was applied via pluronic gel directly after the injury of the left carotid artery in mice and the re-endothelialized area was measured after 3 days. After silencing of Rbm38, re-endothelialization was significantly increased as compared to the control siRNA group (*Figure 1E, F*).

3.3 MiR-98 and let-7f are upstream regulators of Rbm38 and mimic the effects of Rbm38 silencing

To better understand the regulatory potential of Rbm38 modulation, we performed bioinformatic assays to screen for binding sites of microRNAs in the Rbm38 3'-UTR by applying the TargetScan database (http://www.targetscan.org).

Here, we identified conserved sites for miR-98-5p and let-7f-5p. Validation experiments by luciferase reporter assays indeed confirmed that the overexpression of both miR-98-5p and let7f-5p led to a significant reduction of luciferase gene reporter activity showing that these two miRNAs are indeed direct regulators of Rbm38 (Supplementary material online, *Figure S4*). Additional experiments demonstrated that the overexpression of both miRNAs together led to a significant reduction in Rbm38 mRNA and protein levels (Supplementary material online, *Figure S5*). Overexpression of these two miRNAs mimicked the effects of Rbm38 silencing and led to an increase in proliferation as well as migration (*Figure 2A, B*). To better understand the beneficial effects on the cell proliferation, we employed cell cycle assays to check for specific alterations of the cell cycle of endothelial cells after miRNA modulation. Here, we found that overexpression of both miRNAs, especially in the combination, led to a significant increase of cells in the S-phase, whereas the number of cells in the G0/G1 phase was significantly decreased (*Figure 2C, D*). From the oncology field is known that Rbm38 has a role in the stabilization of the cell cycle inhibitor p21.[8,25] Indeed we found silencing of Rbm38 to significantly inhibit p21 levels which was also mimicked by overexpression of the two regulating miRNAs miR-98 and let-7f (Supplementary material online, *Figure S6*). As also other factors are assumed to influence Rbm38 biology, we performed a proteome analysis of HUVECs in an immunoprecipitation approach investigating Rbm38 interacting factors via mass spectrometry (Supplementary material online, *Table S2*) as well as a proteome analysis after Rbm38 silencing (Supplementary material online, *Figure S7* and *Table S3*) showing several affected proteins. We also tried to gain more insight for miR-98/let7f signalling via the use of additional luciferase reporter assays for direct miR targets predicted from TargetScan data base and revealed HMGA2 and FGF5 to be direct targets of miR-98/let7f (Supplementary material online, *Figure S8*).

We next translated our *in vitro* observations into a relevant *in vivo* model. Here, we observed that local overexpression of these two miRNAs (which were mixed with pluronic gels) within injured carotid arteries triggered a significant increase in re-endothelialization capacity (*Figure 2E, F*). This observation suggests that both Rbm38 silencing and overexpression of the two Rbm38-regulating miRNAs is a novel therapeutic approach to improve carotid healing e.g. after stent implantations or operations.

4. Discussion

The present study identified novel biological functions of Rbm38 in endothelial biology. Silencing of Rbm38 improved endothelial cell function. *In vivo*, we showed RNA-binding motif protein 38 and its upstream regulators miR-98 and let-7f to be crucially involved in re-endothelialization after arterial injury.

RNA-binding proteins are important players in the regulation of multiple biological processes and cellular functions, and they are involved in the post-transcriptional regulation of coding and non-coding RNAs. Rbm38 is implicated in the regulation of cell proliferation and cell cycle. It is known to stabilize p21, p73, and HuR by binding to the corresponding mRNA[8,25,26] and to destabilize p63 and p53 transcripts leading to the

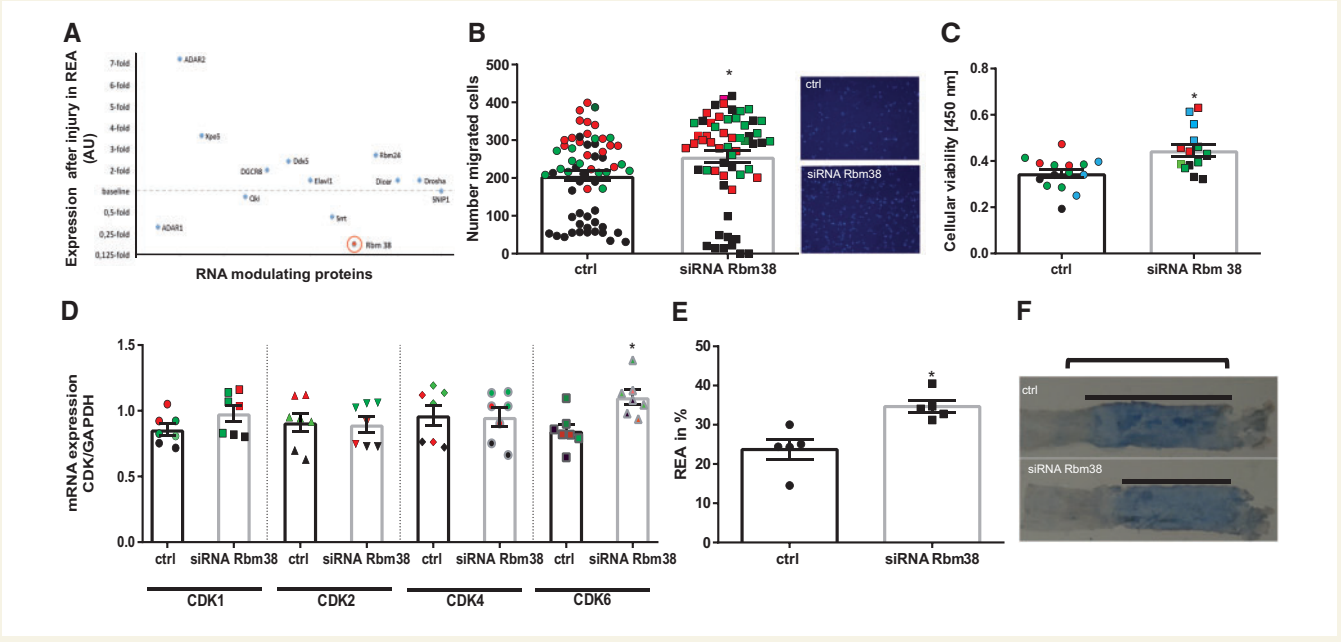

Figure 1 Regulation of Rbm38 during endothelial injury process and its biological functions in endothelial cells *in vitro* and *in vivo*. (*A*) The expression of several RNA-binding proteins was measured in carotid artery after electric injury using qRT-PCR in re-endothelialized and denudated areas. The expression of proteins in denudated area is expressed as baseline. The expression of proteins is indicated as fold change expression in re-endothelialized area in comparison to the baseline expression in denudated areas. $n = 3–5$ animals. (*B*) Number of migrated cells was measured in HUVECs 48 h after silencing of Rbm38 using Boyden chamber assay. $n = 58–63$ biological replicates with each three photographs per well in different locations from three independent experiments. (*C*) The proliferation capacity of endothelial cells (HUVECs) was determined after silencing of Rbm38 via siRNA transfection for 48 h ($n = 15$ biological replicates from four independent experiments). (*D*) Rbm38 regulates the expression of distinct cell cycle genes. qRT-PCR based mRNA expression analysis of cyclin-dependent kinases (CDKs) in HUVECs 48 h after transfection with respective siRNA or control. $n = 7$ biological replicates from three independent experiments. (*E*) The effect of Rbm38 silencing on the re-endothelialization capacity *in vivo*. The re-endothelialization area (%) was determined at day 3 after carotid injury in control group with control siRNA and the treatment group with the application of siRNA Rbm38. $n = 4–5$ mice per group. (*F*) Representative photographs of mice carotid arteries after injury are shown. Initial injury is indicated by a bracket. Denudated area is stained in blue (bar); REA in white. AU, arbitrary units. $^*P < 0.05$. Biological replicates of single independent experiments are uniformly colour-coded. Statistical significance was calculated referring to the biological replicates by unpaired Student's *t*-test.

reduced translation of these proteins.[1,8] In cancer cells Rbm38 fulfils different functions: originally it was described to be an oncogene in gastrointestinal system and malignant lymphomas as well as in breast and prostate cancer.[12,27,28] Recent studies suggest that Rbm38 can also operate as a tumour suppressor.[9,10,29] Rbm38 is known to be expressed in hematopoietic organs (bone marrow, spleen and thymus). Our results show that Rbm38 is also expressed in vascular cells, whereby its expression is significantly higher in endothelial cells compared to smooth muscle cells (Supplementary material online, *Figure S9*). In endothelial cells, it is localized to a large extent in the cytosol (Supplementary material online, *Figure S10*). Furthermore, silencing of Rbm38 in vascular cells inhibits p21 levels leading to modifications of endothelial cell activity during the cell cycle.

Mice deficient in Rbm38 exhibit signs of accelerated aging and develop haematopoietic defects as well as spontaneous tumours.[13] Under hypoxic conditions Rbm38 decreases the level of HIF1a protein in human tumour cells.[25] Increased HIF1a levels promote tumour growth and angiogenesis.[30] These data suggest a protective role of Rbm38 in diverse cancer cells. Our data indicate that Rbm38 is highly expressed in endothelial cells and inversely correlates with the proliferative characteristics of endothelial cells exhibiting its anti-proliferative properties. As the role of Rbm38 in cell cycle and its function in the stabilization of the cell cycle inhibitor p21 is known from the oncology field,[6] we also found that overexpression of miR-98-5p and let-7f-5p let to a significant increase of endothelial cells in the S-phase. Additionally, the overexpression of the two regulating miRNAs miR-98-5p and let-7f-5p mimicked the effect of silencing of Rbm38 on the p21 level. Notably, we validated these *in vitro* data also *in vivo* by showing that local overexpression of miR-98-5p and let-7f-5p in pluronic gel applied to injured arteries let to a significant increase in re-endothelialization capacity.

Additionally, we revealed that not only miRNAs are key factors for modulating Rbm38 biology. Our data showed several enriched and/or deregulated proteins which could be of potential interest for further studies. We also indicated the interaction between miR-98/let-7f and HMGA2 as well as FGF5. Such regulation could, therefore, support miRNA action in our endothelial model system, e.g. chromatin modification. FGF5 is known to be involved in the process of cell proliferation, tissue repair, and cell differentiation[31–33] and HMGA2 plays a role in chromosomal organization and transcriptional regulation influencing cell proliferation in chondrocytes and adipose tissue-derived stem cells and positively regulates the cell response after DNA damage in cancer cells.[34,35] Such ideas could be followed-up in future studies investigating these miR effectors in the context of EC biology.

Activation of re-endothelialization after arterial injury is known to attenuate neointima formation.[36–38] Therefore, new therapeutic strategies are necessary to improve the endothelial function after vascular injuries in

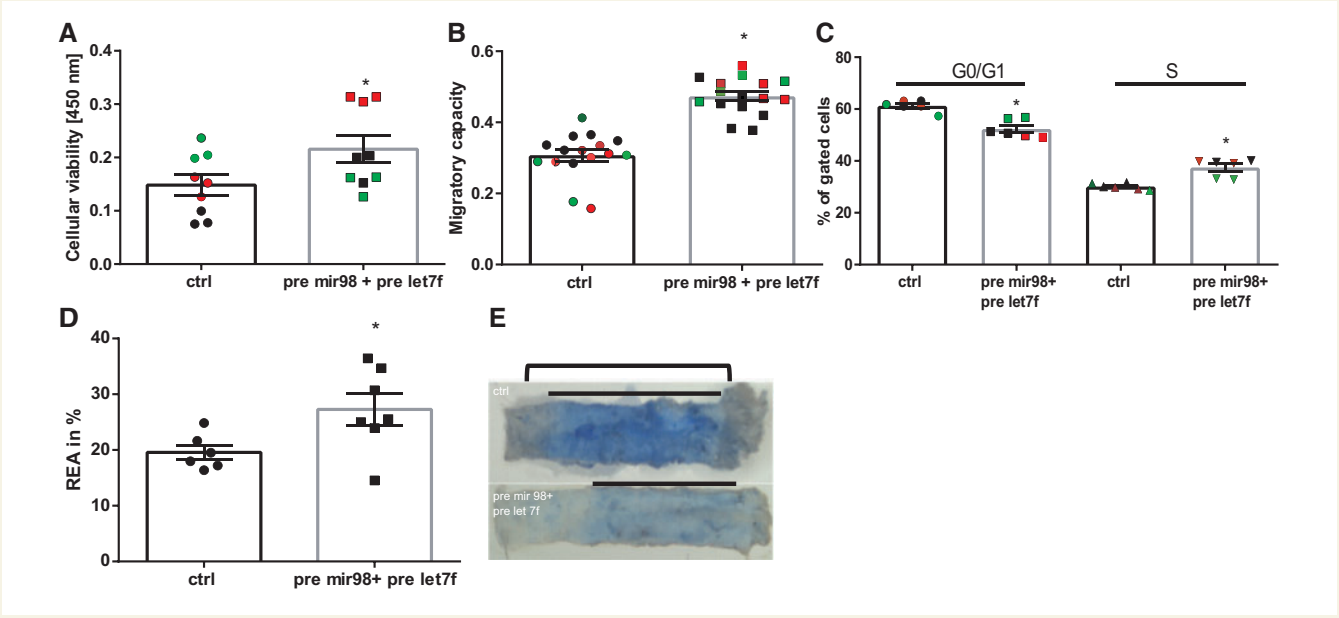

Figure 2 Overexpression of pre-miR-98 and pre-let7f has positive effects in endothelial cells and mimics the effects of Rbm38 silencing. (*A*) The proliferative capacity of HUVECs was measured 48 h after co-transfection with pre-miR-98 and pre-let7f in HUVECs and detected by WST-1 viability assay. $n = 9$ biological replicates from three independent experiments. (*B*) The migration capacity of HUVECs was measured by the use of scratch wounding assay 48 h after co-transfection with pre-miR-98 and pre-let7f in HUVECs. The migratory index was determined after 6 h. $n = 16$ biological replicates from three independent experiments. (*C*) The effect of the overexpression of pre-miR-98 and pre-let7f after 48 h on the cell cycle was detected in endothelial cells in S phase and in G0/G1 phase by FACS analysis. $n = 6$ biological replicates from three independent experiments. (*D*) Overexpression of pre-miR-98 and pre-let7f affects re-endothelialization *in vivo*. The re-endothelialization area (%) was determined at day 3 after carotid injury in the control group with control miRNA and the treatment group with the application of pre-miR-98 and pre-let-7f via pluronic gel. $n = 6$–7 animals. (*E*) Representative photographs of mice carotid arteries after injury are shown. Initial injury is indicated by a bracket. Denudated area is stained in blue (bar); Re-endothelialized area (REA) in white. AU, arbitrary units. $^*P < 0.05$. Biological replicates of single independent experiments are uniformly colour-coded. Statistical significance was calculated referring to the biological replicates by unpaired Student's *t*-test.

the context of percutaneous coronary interventions (PCI) procedures. The local delivery of the miRNAs and siRNAs via pluronic gel applied in this study represents a new alternative treatment option in comparison to a systemic application of therapeutics. The local application of siRNA or miRNAs has the advantage of less systemic side effects, and therefore, could be used locally, e.g. as a coating of balloons or stents in the course of coronary or peripheral interventions to improve the re-endothelialization after arterial injury. There is a promising therapeutic method to apply drugs directly and non-systemically through blood vessel walls into adventitial tissues in patients with peripheral artery disease (DANCE study, ClinicalTrials.gov Identifier: NCT01983449). For that purpose it would also be conceivable to apply the siRNAs or miRNAs of interest in this way to influence the vascular healing after arterial injury.

Collectively, we describe for the first time the role of Rbm38 as a key player in the re-endothelialization process after an arterial injury. Mechanistically, we demonstrate that the local inhibition of Rbm38 or the overexpression of miR-98 and let-7f improve proliferative features of the endothelial cells and is responsible for the positive effects of the re-endothelialization capacity after arterial injury. Since silencing of Rbm38 and overexpression of miR-98 and let-7f were able to improve the regeneration of the endothelium it could be a promising therapeutic target to improve the re-endothelialization after balloon angioplasty in a clinical scenario, especially regarding the absent systemic side effects due to the local delivery of the therapeutics.

Supplementary material

Supplementary material is available at *Cardiovascular Research* online.

Conflict of interest: T.T. has filed patents in the field of non-coding RNAs and holds shares of Cardior Pharmaceuticals GmbH. Other authors have no conflicts of interest.

Funding

This work was supported by the Deutsche Herzstiftung [S/03/13 to K.S.] and the Fondation Leduqc (MIRVAD) (to T.T.).

References

1. Leveille N, Elkon R, Davalos V, Manoharan V, Hollingworth D, Oude Vrielink J, Le Sage C, Melo CA, Horlings HM, Wesseling J, Ule J, Esteller M, Ramos A, Agami R. Selective inhibition of microRNA accessibility by RBM38 is required for p53 activity. *Nat Commun* 2011;**2**:513.
2. Kim MY, Hur J, Jeong S. Emerging roles of RNA and RNA-binding protein network in cancer cells. *BMB Rep* 2009;**42**:125–130.
3. Thum T, Gross C, Fiedler J, Fischer T, Kissler S, Bussen M, Galuppo P, Just S, Rottbauer W, Frantz S, Castoldi M, Soutschek J, Koteliansky V, Rosenwald A, Basson MA, Licht JD, Pena JT, Rouhanifard SH, Muckenthaler MU, Tuschl T, Martin GR, Bauersachs J, Engelhardt S. MicroRNA-21 contributes to myocardial disease by stimulating MAP kinase signalling in fibroblasts. *Nature* 2008;**456**:980–984.
4. Vidigal JA, Ventura A. The biological functions of miRNAs: lessons from *in vivo* studies. *Trends Cell Biol* 2015;**25**:137–147.
5. Thum T, Condorelli G. Long noncoding RNAs and microRNAs in cardiovascular pathophysiology. *Circ Res* 2015;**116**:751–762.

6. Miyamoto S, Hidaka K, Jin D, Morisaki T. RNA-binding proteins Rbm38 and Rbm24 regulate myogenic differentiation via p21-dependent and -independent regulatory pathways. *Genes Cells* 2009;**14**:1241–1252.
7. Cho SJ, Zhang J, Chen X. RNPC1 modulates the RNA-binding activity of, and cooperates with, HuR to regulate p21 mRNA stability. *Nucleic Acids Res* 2010;**38**:2256–2267.
8. Shu L, Yan W, Chen X. RNPC1, an RNA-binding protein and a target of the p53 family, is required for maintaining the stability of the basal and stress-induced p21 transcript. *Genes Dev* 2006;**20**:2961–2972.
9. Xue JQ, Xia TS, Liang XQ, Zhou W, Cheng L, Shi L, Wang Y, Ding Q. RNA-binding protein RNPC1: acting as a tumor suppressor in breast cancer. *BMC Cancer* 2014;**14**: 322. 322-2407-14-322.
10. Ding C, Cheng S, Yang Z, Lv Z, Xiao H, Du C, Peng C, Xie H, Zhou L, Wu J, Zheng S. Long non-coding RNA HOTAIR promotes cell migration and invasion via down-regulation of RNA binding motif protein 38 in hepatocellular carcinoma cells. *Int J Mol Sci* 2014;**15**:4060–4076.
11. Ye J, Liang R, Bai T, Lin Y, Mai R, Wei M, Ye X, Li L, Wu F. RBM38 plays a tumor-suppressor role via stabilizing the p53-mdm2 loop function in hepatocellular carcinoma. *J Exp Clin Cancer Res* 2018;**37**:212. 212-018-0852-x.
12. Hotte GJ, Linam-Lennon N, Reynolds JV, Maher SG. Radiation sensitivity of esophageal adenocarcinoma: the contribution of the RNA-binding protein RNPC1 and p21-mediated cell cycle arrest to radioresistance. *Radiat Res* 2012; **177**:272–279.
13. Zhang J, Xu E, Ren C, Yan W, Zhang M, Chen M, Cardiff RD, Imai DM, Wisner E, Chen X. Mice deficient in Rbm38, a target of the p53 family, are susceptible to accelerated aging and spontaneous tumors. *Proc Natl Acad Sci U S A* 2014;**111**: 18637–18642.
14. van den Hoogenhof MMG, van der Made I, Beqqali A, de Groot NE, Damanafshan A, van Oort RJ, Pinto YM, Creemers EE. The RNA-binding protein Rbm38 is dispensable during pressure overload-induced cardiac remodeling in mice. *PLoS One* 2017; **12**:e0184093.
15. Zhang J, Xu E, Ren C, Yang HJ, Zhang Y, Sun W, Kong X, Zhang W, Chen M, Huang E, Chen X. Genetic ablation of Rbm38 promotes lymphomagenesis in the context of mutant p53 by downregulating PTEN. *Cancer Res* 2018;**78**:1511–1521.
16. Bohm F, Pernow J. The importance of endothelin-1 for vascular dysfunction in cardiovascular disease. *Cardiovasc Res* 2007;**76**:8–18.
17. Roberts AC, Porter KE. Cellular and molecular mechanisms of endothelial dysfunction in diabetes. *Diab Vasc Dis Res* 2013;**10**:472–482.
18. Erdmann J, Junemann J, Schroder A, Just I, Gerhard R, Pich A. Glucosyltransferase-dependent and -independent effects of TcdB on the proteome of HEp-2 cells. *Proteomics* 2017;**17**:doi:10.1002/pmic.201600435.
19. Cox J, Mann M. MaxQuant enables high peptide identification rates, individualized p.p.b.-range mass accuracies and proteome-wide protein quantification. *Nat Biotechnol* 2008;**26**:1367–1372.
20. Cox J, Neuhauser N, Michalski A, Scheltema RA, Olsen JV, Mann M. Andromeda: a peptide search engine integrated into the MaxQuant environment. *J Proteome Res* 2011;**10**:1794–1805.
21. Tyanova S, Temu T, Sinitcyn P, Carlson A, Hein MY, Geiger T, Mann M, Cox J. The Perseus computational platform for comprehensive analysis of (prote)omics data. *Nat Methods* 2016;**13**:731–740.
22. Brouchet L, Krust A, Dupont S, Chambon P, Bayard F, Arnal JF. Estradiol accelerates reendothelialization in mouse carotid artery through estrogen receptor-alpha but not estrogen receptor-beta. *Circulation* 2001;**103**:423–428.
23. Carmeliet P, Moons L, Stassen JM, De Mol M, Bouche A, van den Oord JJ, Kockx M, Collen D. Vascular wound healing and neointima formation induced by perivascular electric injury in mice. *Am J Pathol* 1997;**150**:761–776.
24. Sonnenschein K, Horvath T, Mueller M, Markowski A, Siegmund T, Jacob C, Drexler H, Landmesser U. Exercise training improves *in vivo* endothelial repair capacity of early endothelial progenitor cells in subjects with metabolic syndrome. *Eur J Cardiovasc Prev Rehabil* 2011;**18**:406–414.
25. Cho SJ, Teng IF, Zhang M, Yin T, Jung YS, Zhang J, Chen X. Hypoxia-inducible factor 1 alpha is regulated by RBM38, a RNA-binding protein and a p53 family target, via mRNA translation. *Oncotarget* 2015;**6**:305–316.
26. Yan W, Zhang J, Zhang Y, Jung YS, Chen X. p73 expression is regulated by RNPC1, a target of the p53 family, via mRNA stability. *Mol Cell Biol* 2012;**32**:2336–2348.
27. Zhang J, Cho SJ, Shu L, Yan W, Guerrero T, Kent M, Skorupski K, Chen H, Chen X. Translational repression of p53 by RNPC1, a p53 target overexpressed in lymphomas. *Genes Dev* 2011;**25**:1528–1543.
28. Bar-Shira A, Pinthus JH, Rozovsky U, Goldstein M, Sellers WR, Yaron Y, Eshhar Z, Orr-Urtreger A. Multiple genes in human 20q13 chromosomal region are involved in an advanced prostate cancer xenograft. *Cancer Res* 2002;**62**:6803–6807.
29. Huang W, Wei XL, Ni W, Cao M, Meng L, Yang H. The expression of RNA-binding protein RBM38 decreased in renal cell carcinoma and represses renal cancer cell proliferation, migration, and invasion. *Tumour Biol* 2017;**39**: doi:1010428317701635.
30. Harris AL. Hypoxia–a key regulatory factor in tumour growth. *Nat Rev Cancer* 2002; **2**:38–47.
31. Zhan X, Bates B, Hu XG, Goldfarb M. The human FGF-5 oncogene encodes a novel protein related to fibroblast growth factors. *Mol Cell Biol* 1988;**8**:3487–3495.
32. Itoh N, Ornitz DM. Fibroblast growth factors: from molecular evolution to roles in development, metabolism and disease. *J Biochem* 2011;**149**:121–130.
33. Liu D, Zhang C, Li X, Zhang H, Pang Q, Wan A. MicroRNA-567 inhibits cell proliferation, migration and invasion by targeting FGF5 in osteosarcoma. *EXCLI J* 2018;**17**:102–112.
34. Richter A, Lubbing M, Frank HG, Nolte I, Bullerdiek JC, von Ahsen I. High-mobility group protein HMGA2-derived fragments stimulate the proliferation of chondrocytes and adipose tissue-derived stem cells. *Eur Cell Mater* 2011;**21**:355–363.
35. Summer H, Li O, Bao Q, Zhan L, Peter S, Sathiyanathan P, Henderson D, Klonisch T, Goodman SD, Droge P. HMGA2 exhibits dRP/AP site cleavage activity and protects cancer cells from DNA-damage-induced cytotoxicity during chemotherapy. *Nucleic Acids Res* 2009;**37**:4371–4384.
36. Curcio A, Torella D, Indolfi C. Mechanisms of smooth muscle cell proliferation and endothelial regeneration after vascular injury and stenting: approach to therapy. *Circ J* 2011;**75**:1287–1296.
37. Daniel JM, Penzkofer D, Teske R, Dutzmann J, Koch A, Bielenberg W, Bonauer A, Boon RA, Fischer A, Bauersachs J, van Rooij E, Dimmeler S, Sedding DG. Inhibition of miR-92a improves re-endothelialization and prevents neointima formation following vascular injury. *Cardiovasc Res* 2014;**103**:564–572.
38. Dutzmann J, Koch A, Weisheit S, Sonnenschein K, Korte L, Haertle M, Thum T, Bauersachs J, Sedding DG, Daniel JM. Sonic hedgehog-dependent activation of adventitial fibroblasts promotes neointima formation. *Cardiovasc Res* 2017;**113**:1653–1663.